

## Heat Transfer to Large Objects in Large Pool Fires

B. L. Bainbridge and N. R. Keltner

Thermal Test and Analysis Division(7537), Sandia National Laboratories,  
P. O. Box 5800, Albuquerque, New Mexico, 87185 (USA)

### Summary

A series of large pool fires has provided temperature and heat flux data for a large, thermally massive object. Lower temperatures were obtained at 4 elevations. Temperature measurements on a large calorimeter were used to obtain heat flux levels at 3 axial stations and 4 angular locations. The tests show large spatial and temporal variations for each test that seem to be largely driven by wind effects. A conditioning analysis was used to extract data at periods of lower wind velocities to allow a comparison between test data and simplified fire models. The conditioned data shows a significantly lower variance and better symmetry around the large calorimeter.

### Introduction

Large pool fires are used at Sandia National Laboratories to expose radioactive material shipping containers to levels of temperature and heat flux required by regulatory agencies. Due to the very nature of outdoor pool fires, a large effort has gone into characterizing the temporal and spatial variability of the thermal environment.

Three tests were performed in the summer of 1983 involving a 9.1 by 18.3 meter pool fire fueled with JP-4 aviation fuel. A calorimeter 1.4 m in diameter by 6.1 m long was used to examine the thermal input to a relatively large, massive object. An examination of temperature and heat flux data emphasizes the effect of even low wind conditions on the overall structure of the fire. In an attempt to examine the thermal environment in the absence of any disturbances, a 'conditioning signal' was used to extract data during periods of low wind.

Heat flux and temperature data obtained from the large pool fire tests is presented and the variation over the surface of the large calorimeter is examined. The application of a conditioning signal is used to reduce the wind induced variance in the heat flux data.

## Fire Test Regulations

Fire tests are typically specified as either a temperature versus time curve or as the equivalent of a radiant environment at a specific temperature. An example of the former is provided by the American Society for Testing and Materials (ASTM) in test method E 119, "Standard Methods of Fire Tests of Building Construction and Materials"[1]. The latter specification is used by several agencies that have regulations regarding the fire testing of radioactive material transportation containers. In general, the requirements involve a 30 minute test with the thermal environment equivalent to a radiant source of 1075K with an emissivity of at least 0.9 and a surface absorptivity for the test item of 0.8 or greater. A convective component should be equivalent to still air at 1075K. The specific regulations are available in publications from the agencies themselves:

- a. the Department of Energy (DOE)[2], originally published by ERDA, in chapter 0529 of the ERDA manual "Safety Standards for the Packaging of Fissile and Other Radioactive Materials",
- b. the Department of Transportation (DOT)[3] in the Code of Federal Regulations (CFR) as 49 CFR Part 173,
- c. the Nuclear Regulatory Commission (NRC)[4] in 10 CFR Part 71,
- d. the International Atomic Energy Agency (IAEA)[5] published in IAEA Safety Standards, Safety Series No. 6, "Regulations for the Safe Transport of Radioactive Materials".

A more severe test requirement, E-5 P-191 entitled "Determining Effects of Large Hydrocarbon Pool Fires on Structural Members and Assemblies", has been proposed by the ASTM[6] for evaluating fire protection materials for the petrochemical industry. It requires a thermal environment equivalent to a 1290K source with a 10% convective component. Also stipulated is the rapid development of both high temperatures and heat flux levels in order to impose the thermal shock effects that are produced in actual fire environments.

## Test Instrumentation

The three pool fire tests were conducted in a 9.1 by 18.3 by 0.9 meter concrete pool. The 30 minute tests used a layer of JP-4 fuel, approximately 0.22 m thick, that was floated on 0.66 m of water. Instrumentation was mounted in 8 towers, 4 small calorimeters (0.1 m and 0.2 m diameter) and 1 large calorimeter (1.43 m diameter). Data obtained from the large calorimeter is of

primary interest. Figure 1 shows the relative locations of the instrumentation.

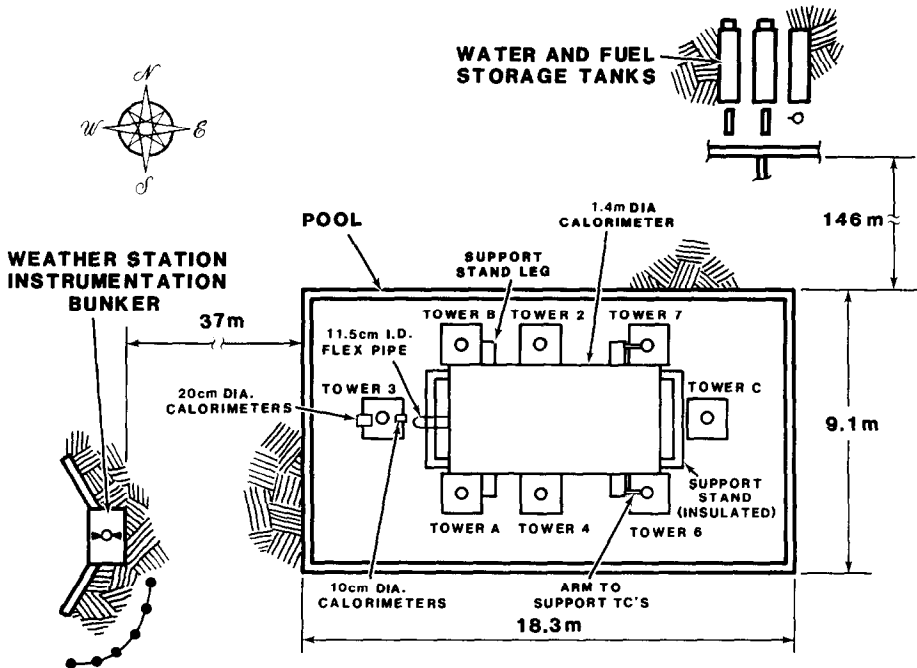


Figure 1. A diagram of the large pool fire facility. Shown are the relative locations of the large calorimeter and towers.

The large calorimeter consisted of a 10 tonne cylinder that was 6.4 m long and 1.4 m in diameter. The 3.2 cm thick walls were of A517 steel and reinforced by 5.1 cm thick ribs located on 61 cm centers. The ends of the cylinder were sealed with plates 1.3 cm thick. The interior of the calorimeter was insulated with 3 layers of 2.5 cm thick material that were held in place with a steel mesh. The large calorimeter was centrally located with its lower surface 0.9 m above the pool surface. Figure 2 shows the physical layout of the large calorimeter.

Type K thermocouples were mounted at 3 axial stations on the large calorimeter: in the middle and at 0.46 m from both ends. At each station, thermocouples were mounted at 4 angular locations: 0(bottom), 90(south), 180(top), and 270(north). At least 3 thermocouples were located at each of the 12 measurement locations. One was mounted between the first and second layers of insulation, the next was an intrinsic thermocouple welded to the inner surface of the cylinder wall, and an exterior thermocouple was mounted with the junction approximately 5 cm from the outer surface(see figure 2). The interior

thermocouples are used to calculate net heat flux and the exterior measurement is used to monitor flame temperatures near the calorimeter surface.

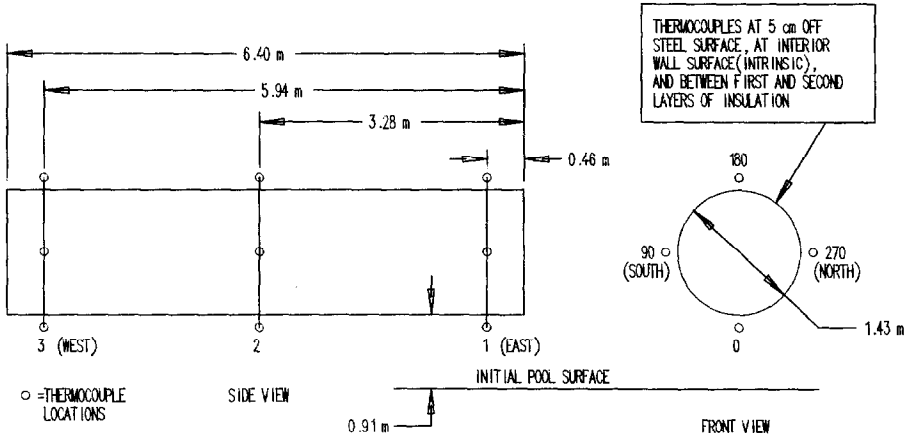


Figure 2. A schematic of the large calorimeter. The axial and circumferential thermocouple locations are shown. Note the cross section that depicts the external, surface, and internal thermocouples.

Temperature measurements in the fire environment were obtained using type K thermocouples mounted on several towers within the pool (figure 1). Towers A, B, and C were 6.1 m in height with measurement stations at 1.42 and 2.62 m above the initial fuel surface. The other 5 towers were 12.2 m tall with thermocouples mounted at 1.42, 2.62, 5.49 and 11.18 m. At all locations, sheathed thermocouples with ungrounded junctions were used.

The data acquisition system consisted of a Hewlett-Packard (HP) 3052A data logger connected to an HP-21 MX computer using fiber optic cables. All channels were recorded every 4.5 seconds. In order to monitor the integrity of the thermocouple channels, a resistance measurement was substituted for the temperature measurement every tenth reading.

Additional details regarding the test instrumentation are available from reference 7. Included is information on the small calorimeters and wind velocity measurements.

## Results

### Temperature Measurements

A complete presentation of all the data recorded during the 3 pool fire tests is beyond the scope of this paper. Representative samples of temperature and heat flux data will be presented with an emphasis placed on examining the variability of heat flux levels. A more complete report is presented in reference 7.

The primary cause of large fluctuations in the fire environment is wind. It induces changes in the mixing and combustion of fuel and air and in the resulting thermal profiles above the fuel surface. The regions of flame above a fire shift location as a function of the wind velocity and the buoyancy induced flow within the fire. Figure 3 shows a sample of recorded wind speed and direction from the third test (test C). The steady rise in speed coupled with the shift in direction of 180 degrees produces a fairly unpredictable environment. Objects in the fire are alternately engulfed in flame and exposed to ambient air.

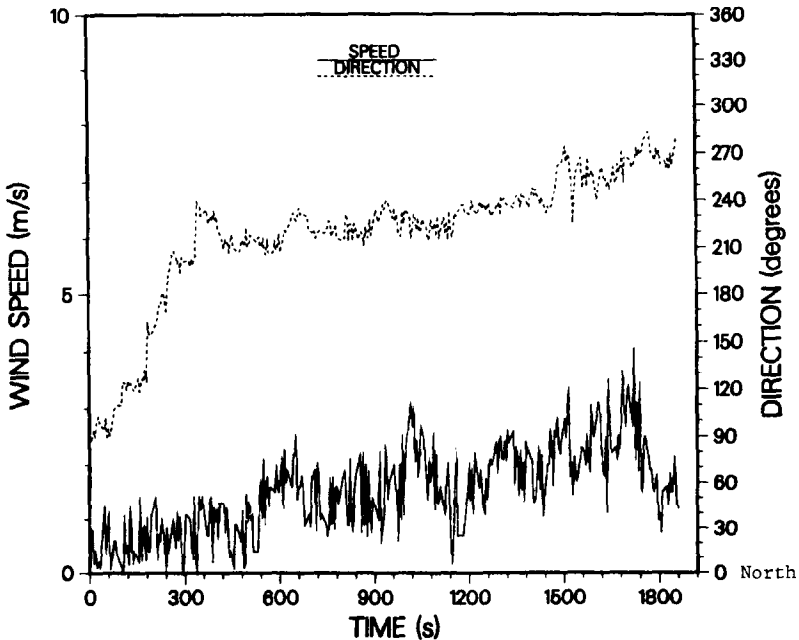


Figure 3. A sample wind velocity plot from test C. The upper trace shows wind direction and the lower wind speed. Note the 180 degree wind shift over the course of the test.

Temperatures recorded from the tower instrumentation clearly show the large fluctuations experienced during the three tests. Figure 4 is a representative sample of temperature versus time for tower 6 (see figure 1) of test A. The temperatures are shown at all 4 heights: from 1.42 m to 11.18 m. While the trend was for lower temperatures with increasing height, there were some periods when all locations registered similar temperatures (1600 to 2000 seconds).

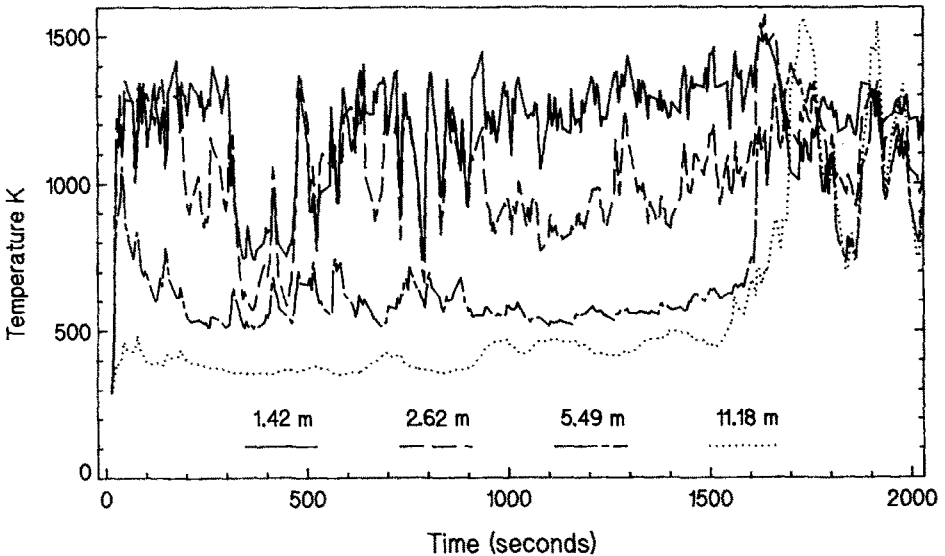


Figure 4. Tower temperature versus height for test A, tower 6.

Another example of the variance in the fire temperature data may be seen in figure 5, where temperatures are plotted for 3 different towers at the same elevation from test C. Tower B has a significantly higher average temperature than the other two. In fact, the difference in temperature approaches 800K. Obviously, the fire was highly asymmetric for most of the test duration.

Tower temperatures are useful for examining the gross fire structure and providing insight regarding the highly variable nature of the temperature profile and heat loads. Table 1 is a compilation of average and standard deviations for tower temperatures recorded during all three tests. Note the decreasing average and increasing standard deviation with increasing elevation. Even at the lowest elevation, 1.42 m, the standard deviation is 20% and it increases to over 60% at 11.18 m. As a result of these large variations, objects within the fire could see heat loads that would vary by a factor of two or more depending on location.

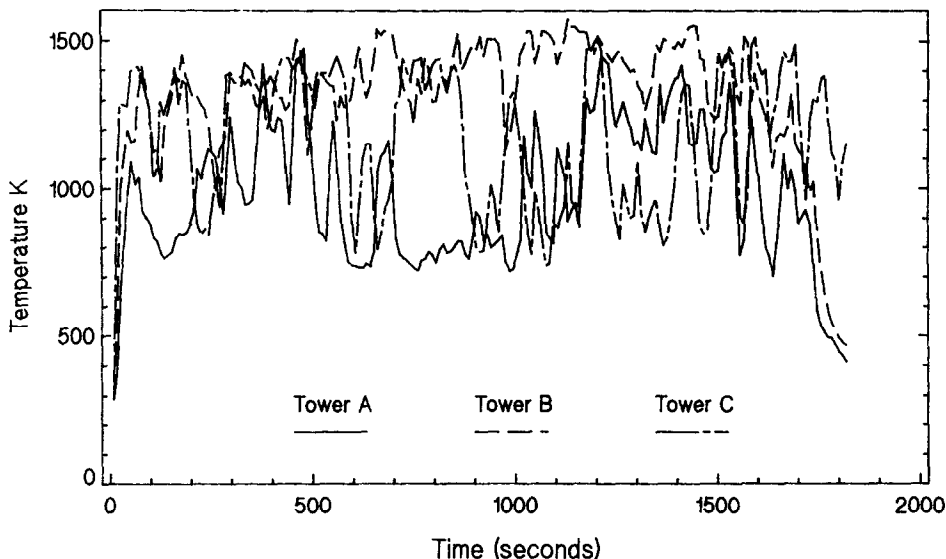


Figure 5. Tower temperatures recorded from test C for 3 different towers. The thermocouples were located at 2.62 m above the initial fuel level.

TABLE 1

Tower temperatures and statistics for tests A, B, and C. The values represent averages obtained over the entire test. Note: the information in this table was obtained from reference 7.

| <u>Location</u>       | <u>Test A</u> | <u>Test B</u> | <u>Test C</u> |
|-----------------------|---------------|---------------|---------------|
| Elevation 1: 1.42 m   |               |               |               |
| Minimum (K)           | 588           | 715           | 446           |
| Maximum (K)           | 1595          | 1532          | 1546          |
| Average (K)           | 1142          | 1194          | 1231          |
| Standard Deviation    | 24%           | 21%           | 18%           |
| Elevation 2: 2.62 m   |               |               |               |
| Minimum (K)           | 393           | 507           | 414           |
| Maximum (K)           | 1575          | 1572          | 1581          |
| Average (K)           | 992           | 1031          | 1094          |
| Standard Deviation(%) | 37%           | 35%           | 32%           |
| Elevation 3: 5.49 m   |               |               |               |
| Minimum (K)           | 346           | 382           | 397           |
| Maximum (K)           | 1529          | 1539          | 1564          |
| Average (K)           | 767           | 829           | 812           |
| Standard Deviation(%) | 52%           | 48%           | 51%           |
| Elevation 4: 11.18 m  |               |               |               |
| Minimum (K)           | 342           | 362           | 326           |
| Maximum (K)           | 1566          | 1494          | 1507          |
| Average (K)           | 649           | 676           | 667           |
| Standard Deviation(%) | 70%           | 61%           | 65%           |

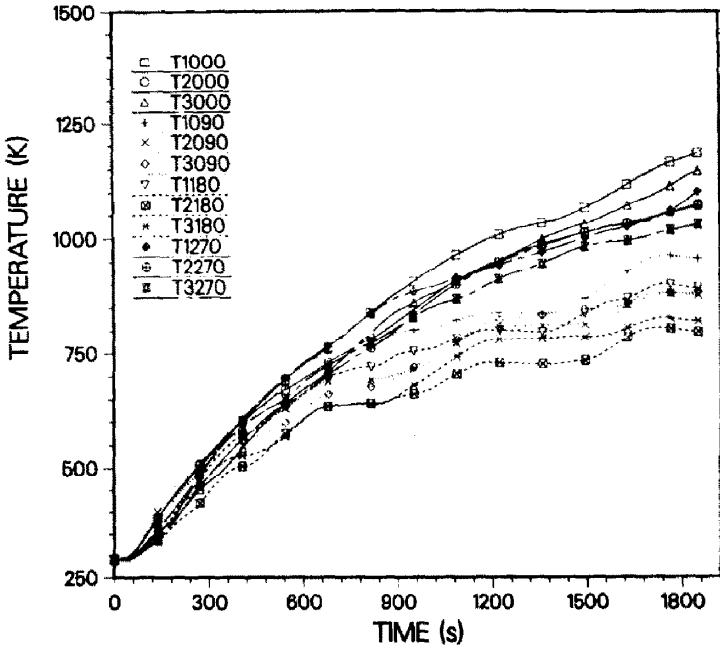


Figure 7. Temperatures measured at the inside surface of the large calorimeter wall for test B.

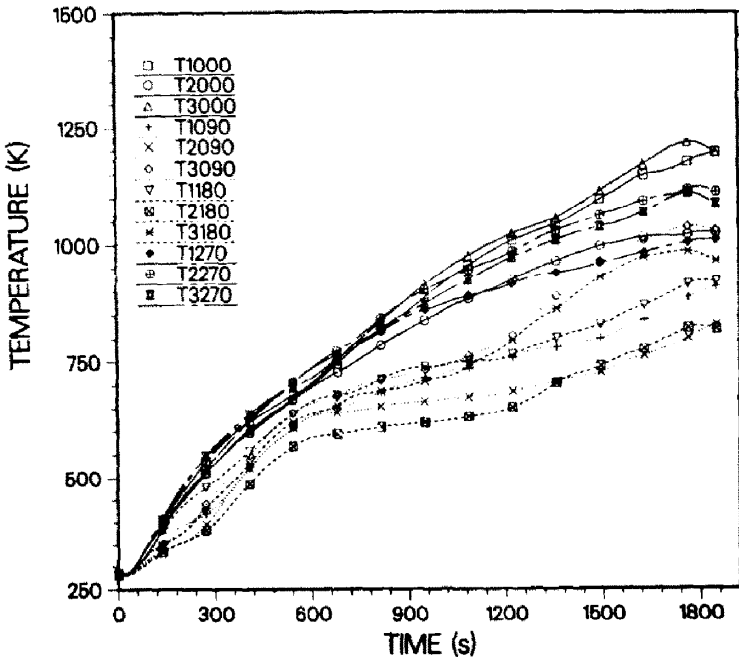


Figure 8. Temperatures measured at the inside surface of the large calorimeter wall for test C.



The large calorimeter provided temperature and heat flux data that is representative of heat loads that would be seen by a massive object in a pool fire. Data recorded from intrinsic thermocouples mounted on the inner surface of the calorimeter wall show the variation in heat loads at different points on the calorimeter body. Figures 6, 7, and 8 show the magnitude of the variation for tests A, B, and C, respectively. An indication of the source of the variance in the data can be seen by comparing the temperatures at 90(south) and 270(north) degrees. In a steady fire environment, a centrally placed object would experience a heat load that would be uniform around the object at a given elevation. As the figures show, the 90 degree locations tend to be much lower than the measurements at 270 degrees. This correlates with the light winds that usually were from the southeast or southwest directions.

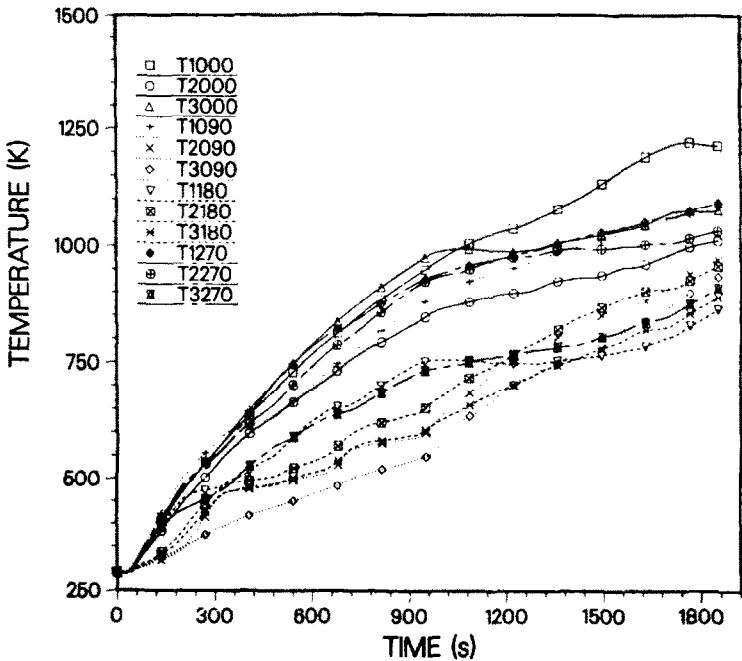


Figure 6. Temperatures measured at the inside surface of the large calorimeter wall for test A.

#### Heat Flux Measurements

The inner surface temperature measurements were used to calculate net surface heat flux for the large calorimeter. A one dimensional inverse heat conduction program, SODDIT(Sandia One Dimensional Direct and Inverse Thermal)[8], was used with a simple model of the calorimeter wall. Temperature

dependent material properties were included. Stability requirements necessitated the use of 4 future times(4 successive data points) for the inverse calculation. This also tends to smooth the data and reduce the noise levels of the resulting output.

One problem with the heat flux calculation was caused when the A517 wall material reached its Curie point(1033K). The abrupt change in thermal properties caused instabilities in the calculated heat flux that are seen as sinusoidal fluctuations. The transition point was reached at different times near the end of the test depending on the temperature history experienced at a particular station on the large calorimeter. A typical point was near 1600 seconds into the test.

Figures 9 and 10 show representative results for test C at station 2, locations 0 and 180, respectively. The inner wall temperature, external gas temperature, and calculated heat flux are all shown as functions of time. Note the difference in frequency content of the three signals. The inner wall temperature changes only very slowly with time and doesn't reflect the rapid fluctuations in the adjacent gas temperature. The calculated heat flux, which is responsive to the derivative of the inner wall temperature, does show some correlation with the gas temperature trace. Note that the negative slope in

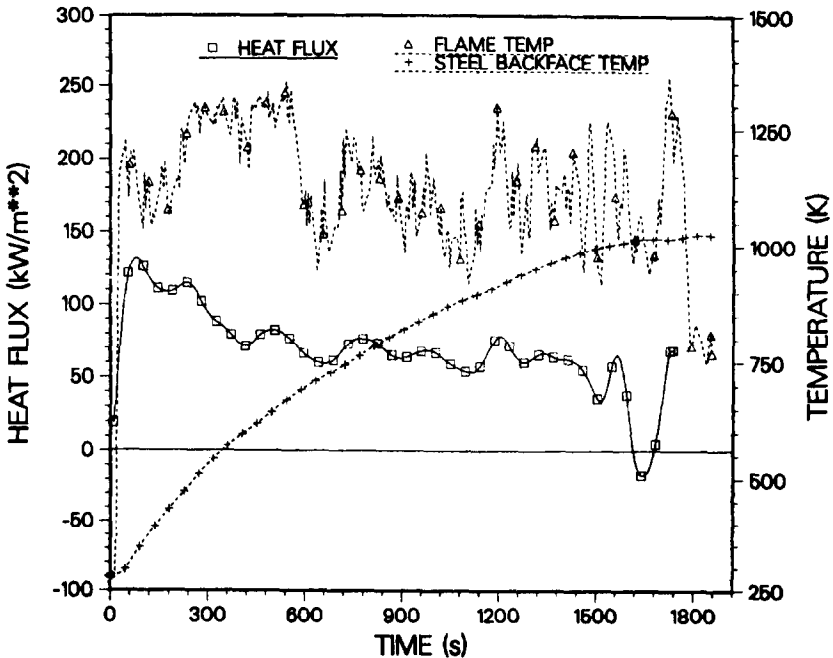


Figure 9. Heat flux, flame temperature and backface temperature for the large calorimeter during test C, station 2, 0 degrees.

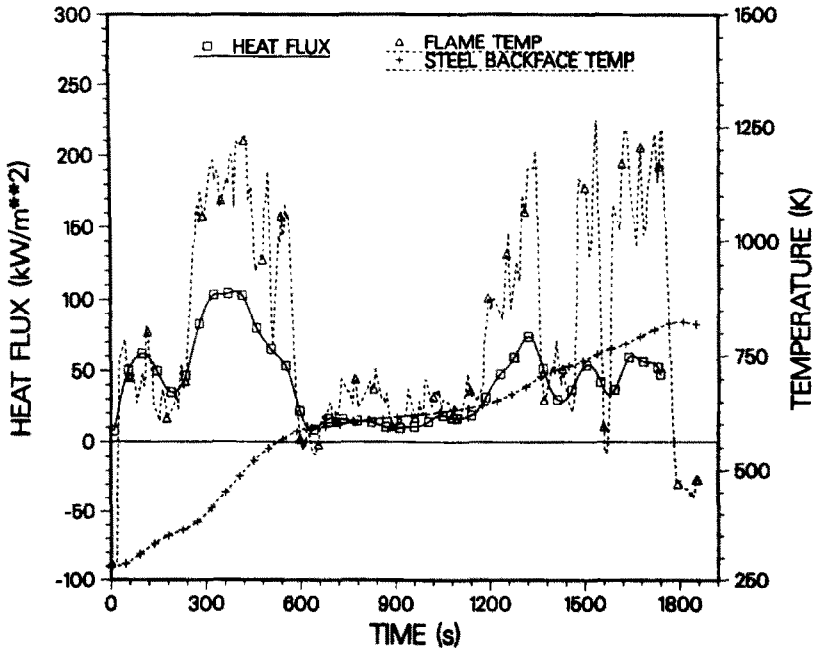


Figure 10. Heat flux, flame temperature and backface temperature for the large calorimeter during test C, station 2, 180 degrees.

figure 9 was due to the rising temperature of the exterior wall of the large calorimeter, which reduced the net heat flux to the wall.

A comparison between figures 9 and 10 shows the large point to point variation in heat flux experienced by the large calorimeter. While the heat flux at 0 degrees remained fairly constant, the more exposed 180 degree location exhibited large changes in heat flux that correlate well with the fluctuations in external gas temperature. This same situation existed for all three tests.

An important aspect of the thermal environment of a fire concerns the distribution of heat flux with location. Fire models typically predict the highest heat flux for the upper surfaces of the cylindrical calorimeter. There has been speculation about the existence of a fuel rich vapor dome near the surface of a large fire[9], although other authors predict its presence only for small (<1 m) diameter fires[10]. The existence of a vapor dome would reduce the heat flux to the lower surface of the calorimeter in accordance with the models. Simplified radiation models base the varying heat flux on the optical path length in a fire and the proximity of the cooler fuel surface to the lower surfaces of an object[11]. To examine the performance of those models, the heat flux histories were averaged over the 3 stations for each test and plotted in figures 11 through 13.

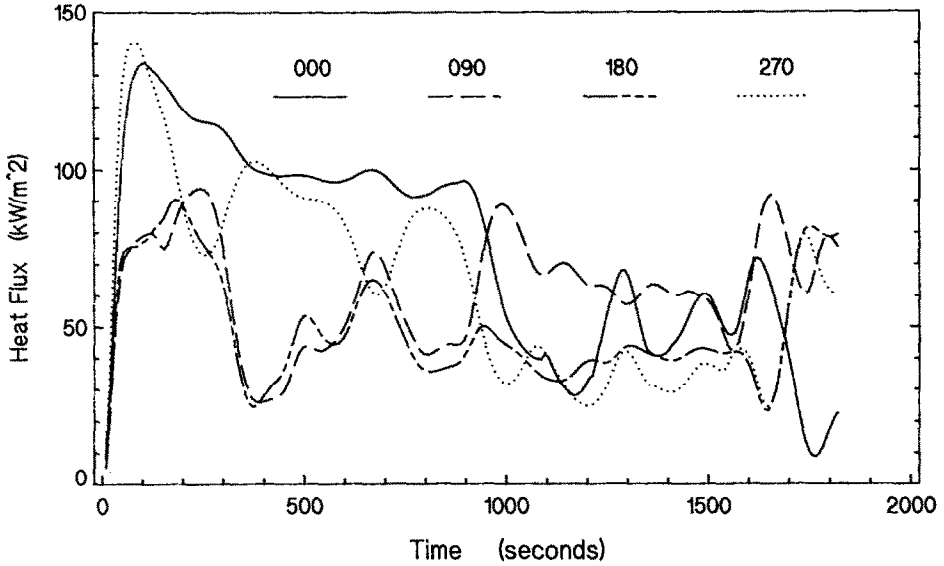


Figure 11. Heat flux versus time for test A. The data was averaged over 3 axial stations.

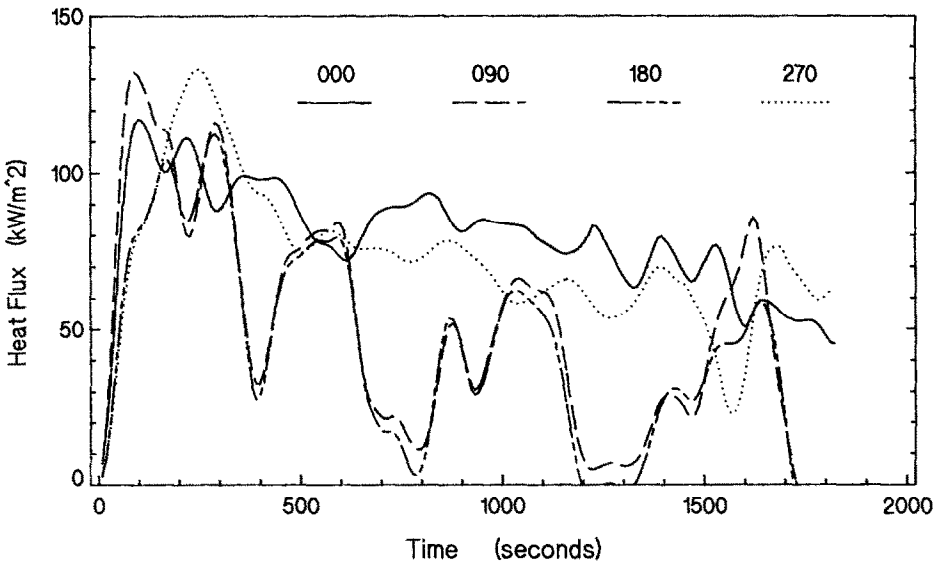


Figure 12. Heat flux versus time for test B. The data was averaged over 3 axial stations.

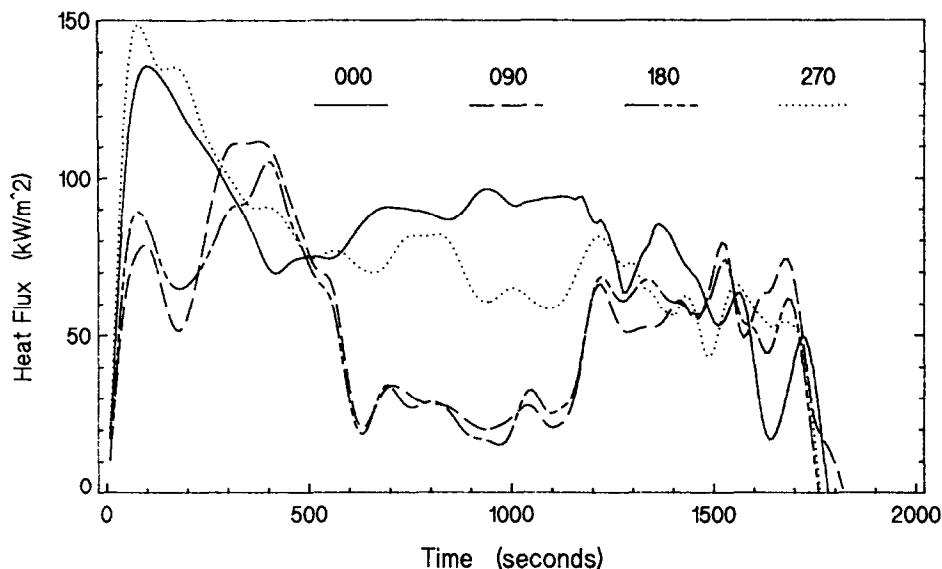


Figure 13. Heat flux versus time for test C. The data was averaged over 3 axial stations.

In all three tests, the data divides itself into two groups: 0 and 270 locations and 90 and 180 locations. This is expected from the generally southerly wind direction experienced during the tests. In other words, the dominant features of the heat flux profiles are wind induced. The variation by angular location is more clearly shown in figures 14 and 15. The total heat flux was estimated by adding a radiated surface heat flux component (emissivity=0.85) to the calculated net heat flux for a given location on the large calorimeter. The total heat flux becomes fairly stationary from a statistical standpoint and the calculated mean value for a given test is more significant. The variation in figure 14 shows the reduction in heat flux for the 90 and 180 locations. The standard deviations for the mean total heat flux values are also greater for the more exposed locations.

A casual inspection of the data seems to indicate a situation opposite to that predicted by the models: the lowest location (0 degrees) has the highest average heat flux while the highest location (180 degrees) has one of the lowest averages. A closer examination shows that the magnitude of the variance in the heat flux data, caused by wind effects, makes it difficult to interpret the distribution of heat flux with location. The data cannot be used in its present form to evaluate the veracity of a particular fire model.

Due to the specification of a fire environment in terms of its radiant equivalent, it is sometimes convenient to present the heat flux data as a function of the surface temperature of the object being tested. Figure 16

shows the heat flux versus calorimeter surface temperature(calculated) averaged over three tests. The behavior as a function of angular location is similar to the plot of heat flux versus time; namely, the 90 and 180 locations show good agreement as do the 0 and 270 locations.

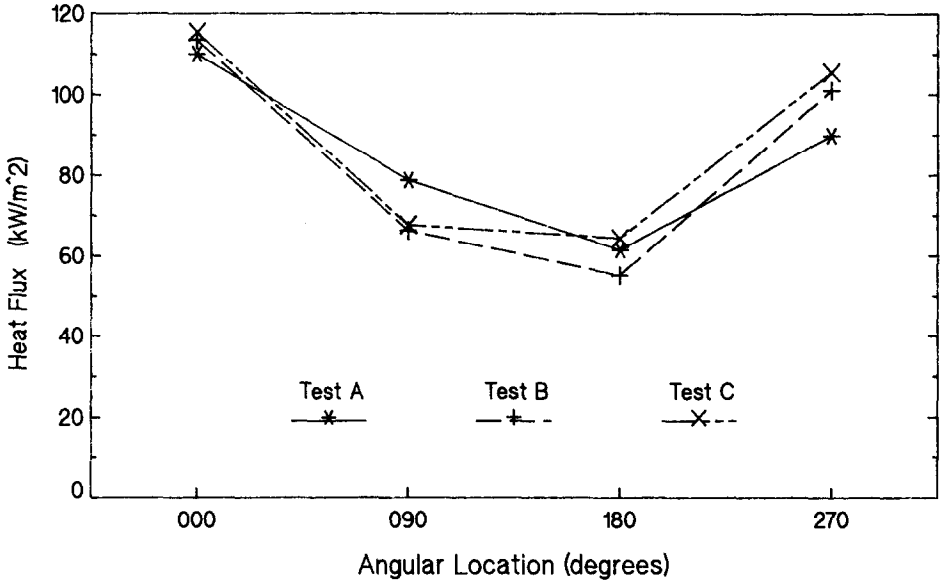


Figure 14. Average total heat flux versus angular location for tests A, B, and C.

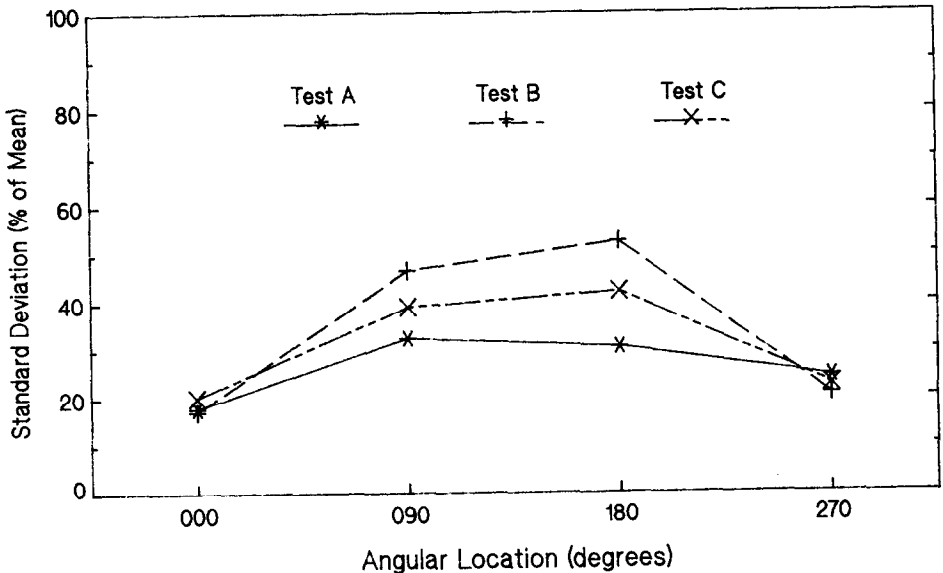


Figure 15. Standard deviations of the average total heat flux versus angular location for tests A, B, and C.

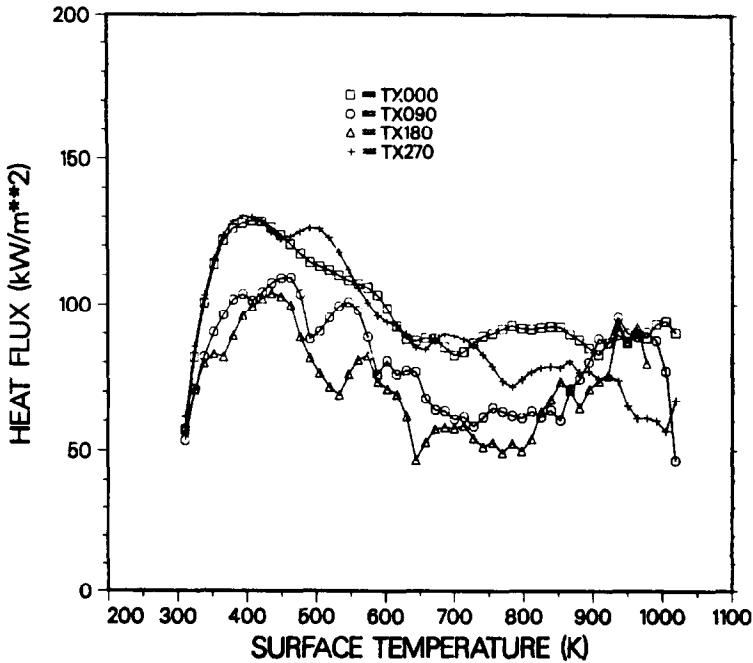


Figure 16. Heat flux versus surface temperature for the large calorimeter. The data was averaged over the three tests and plotted for each angular location.

### Conditional Sampling

Fire models assume the existence of a steady fire environment. It is not possible, at present, to add a non-steady wind component that would allow a comparison to test data. It is desirable, instead, to remove or reduce the impact of data that was recorded during periods of 'significant' wind velocities. Several methods are possible, but one that has been successful is based on the use of tower temperatures to conditionally sample the data. The technique has been employed successfully in the analysis of fire velocities and temperatures[12].

Figure 1 shows that the large calorimeter was surrounded by towers. If an appropriate temperature was selected, it should be possible to examine the data and surmise when a tower was engulfed in flame. If an upwind tower was used, the engulfment of the tower would be an indication of a low wind condition and it would be assumed that the calorimeter was also engulfed. The first difficulty is selecting the temperature for a given height and tower that is an indication of the desired fire condition.

A distribution of all the tower temperatures registered at elevation 2 for all three tests was obtained. Figure 17 shows that the distribution was bimodal: one peak near 730K and another near 1230K. The second peak is assumed

to be the mean value of a second normal distribution that is an indication of a flame present condition. A cutoff temperature of 1040K was used as a conditioning criterion for heat flux data from the large calorimeter to restrict the data set to periods of time when the tower temperatures indicate engulfment. Data was not used if obtained during periods when the upwind tower temperature was below the cutoff point. It was hoped that the wind induced variance in the heat flux data would be reduced.

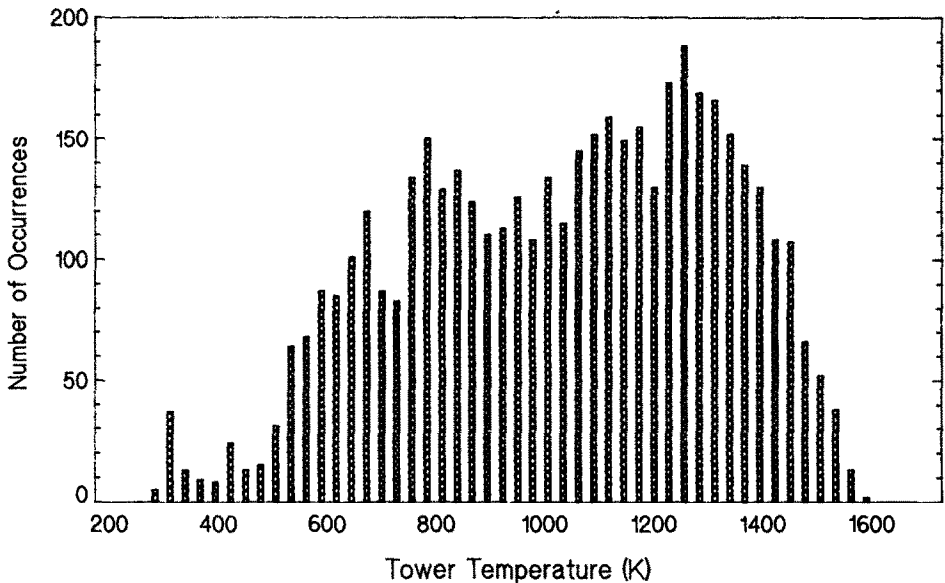


Figure 17. The frequency distribution of tower temperature at 2.62 m. Note the bimodal distribution.

For each test, the flame present temperature was used in conjunction with the data from tower 6, elevation 2, to condition the heat flux data (figures 11 through 13). The results are shown in figures 18 through 20. The heat flux data seems to have a lower variance, especially for the 90 and 180 locations. The effect of conditioning on the statistics is more obvious when presented as a test mean and standard deviation, as was done for the original data set (figures 14 and 15). Again, total heat flux was used and the results plotted in figures 21 and 22. The mean heat flux values begin to show the type of symmetry that would be expected in a steady fire environment: agreement between 90 and 270 locations and the steady change in magnitude from the lowest to highest locations on the calorimeter. Note that the standard deviations are, as expected, much lower for the 90 and 180 locations after being conditioned. The trend in heat flux with location again indicates that the highest values would be found at the bottom of the calorimeter.



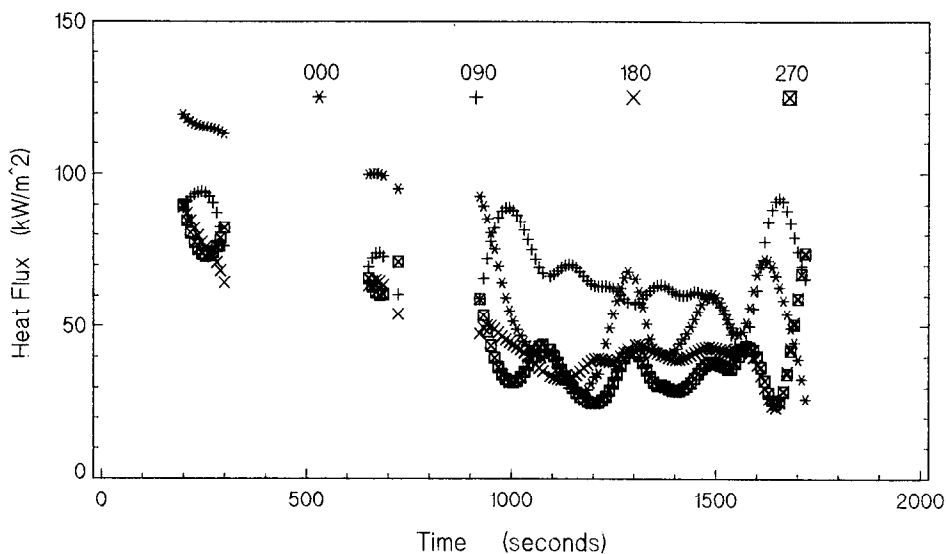


Figure 18. The conditioned data set for test A. Heat flux versus time averaged over 3 stations. The data is plotted as individual points to emphasize the effect of a conditional analysis. The gaps indicate a flame absent condition.

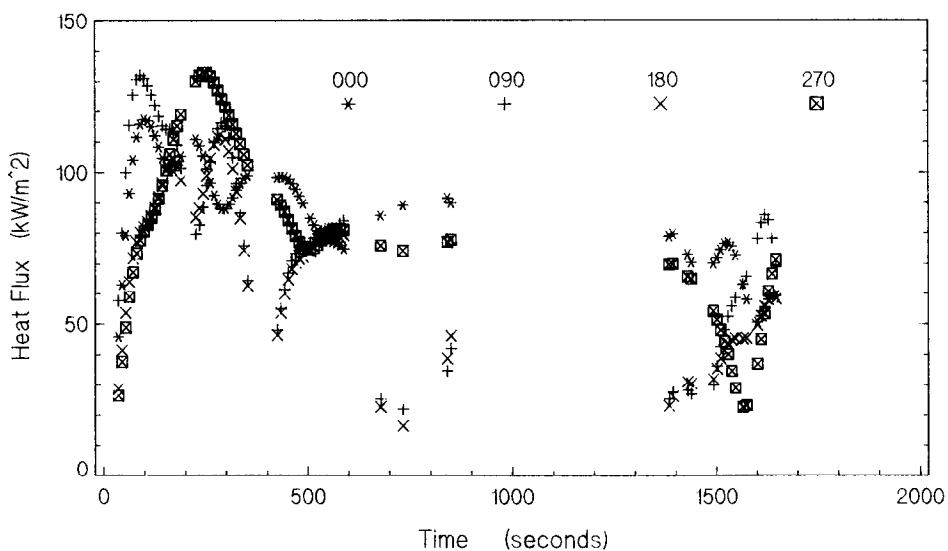


Figure 19. The conditioned data set for test B. Heat flux versus time averaged over 3 stations.

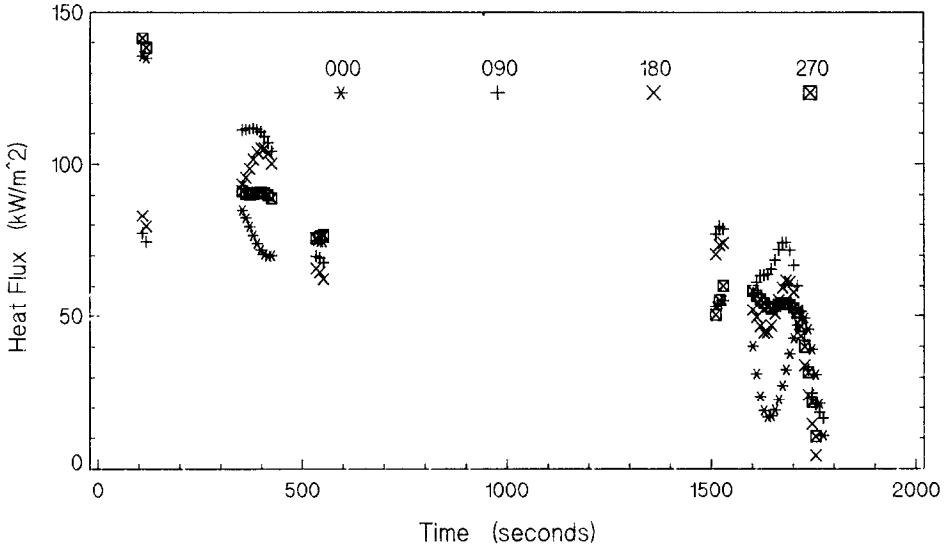


Figure 20. The conditioned data set for test C. Heat flux versus time averaged over 3 stations.

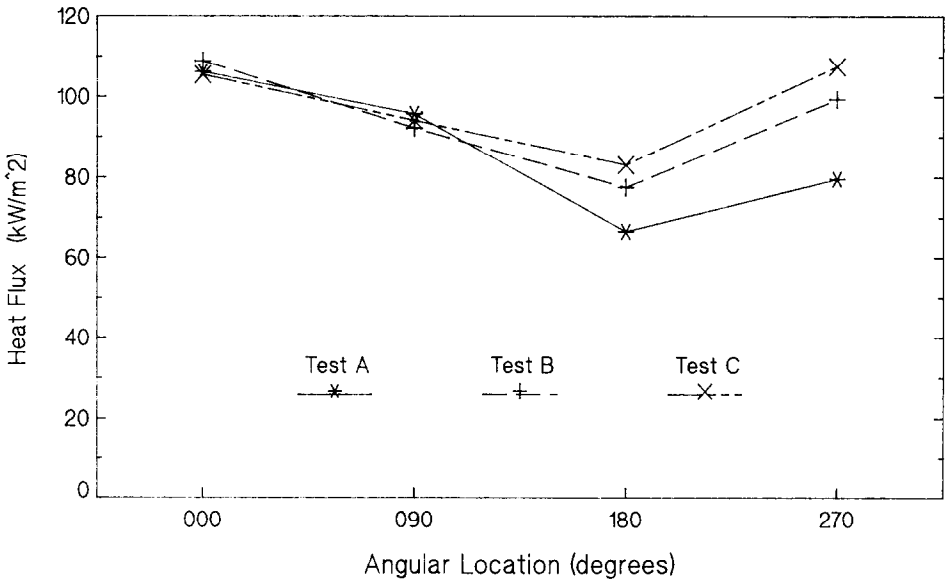


Figure 21. Average total heat flux versus angular location for all tests after applying a conditional analysis. Note how the value for 90 degrees has been increased to a level similar to 270 degrees.

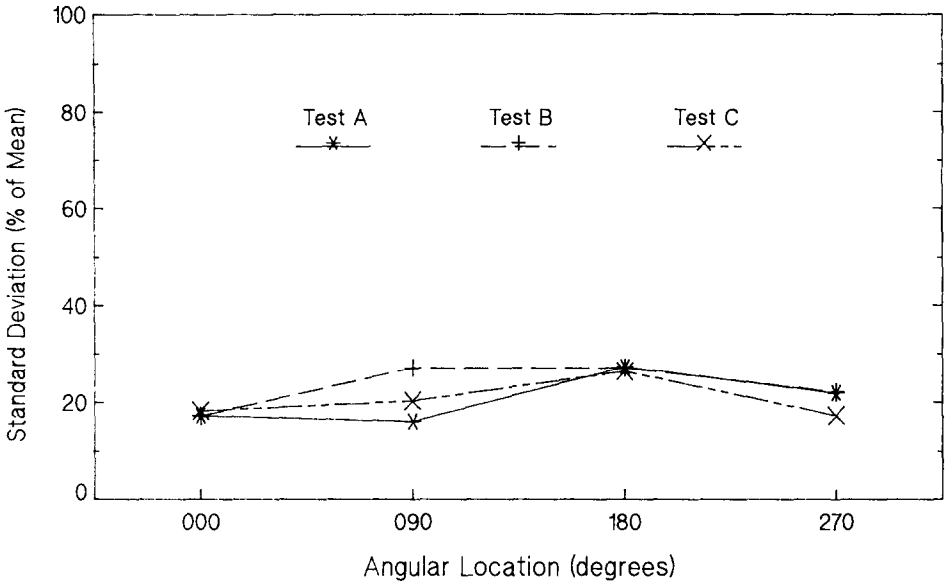


Figure 22. Standard deviation of the average total heat flux after applying a conditional analysis.

It is somewhat surprising that the test statistics are so similar between the three tests, considering the large variance in the original data sets. The mean total heat flux values for locations 0 and 90 are almost identical, although the data does diverge at 180 and 270. This 'collapsing' of the data is another example of the utility of conditioning.

## Conclusions

The thermal environment for a physically large, thermally massive object has been measured in a series of large pool fires. Tower and calorimeter based measurements indicate the large scale fluctuations that are induced by even low velocity winds can mask variations in heat flux as a function of location. The comparison between experimental data and simplified models of the fire becomes difficult.

A conditional analysis has been used to examine the distribution of temperatures and heat flux levels during periods of lower wind velocities. The resulting data set has a much lower variance for locations particularly susceptible to wind effects and the test to test variation is also reduced. Additionally, the total heat flux distribution around the large calorimeter becomes much more symmetric and allows an examination the distribution of heat

flux with location. The technique has also been used successfully in the examination of tower temperatures and fire velocity distributions.

In spite of the large, wind induced variations, average total heat flux exceeded the levels specified in the test regulations for radioactive material shipping containers. This was true for all locations on the large calorimeter.

### Acknowledgments

The authors would like to express their appreciation for the work of J. J. Gregory in the original data analysis. The test program was funded by the Federal Rail Administration of the U.S. Department of Transportation(DOT). This project was directed by the Transportation Technology Center at Sandia National Laboratories. Sandia National Laboratories is operated by AT&T Technologies for the U.S. Department of Energy(DOE) under contract DE-AC04-76DP00789.

### References

1. Standard Methods of Fire Tests of Building Construction and Materials, 1986 Annual Book of ASTM Standards, E 119-83, vol. 4, pp. 353-379.
2. Safety Standards for the Packaging of Fissile and Other Radioactive Materials, United States Energy Research and Development Administration(ERDA) Manual, Chapter 0529, vol. 0000 General Administration, part 0500 Health and Safety.
3. Code of Federal Regulations, Title 49 Transportation, part 173.399, p. 274.
4. Packaging of Radioactive Materials for Transport and Transportation of Radioactive Material Under Certain Conditions, Title 10, Code of Federal Regulations, Part 71, August 19, 1977.
5. Regulations for the Safe Transport of Radioactive Materials, Safety Series No. 6 of International Atomic Energy Safety Standard, 1973 revised edition, IAEA, Vienna, STI/PUB/323.
6. Proposed Test Methods for Determining Effects of Large Hydrocarbon Pool Fires on Structural Members and Assemblies, 1986 Annual Book of ASTM Standards, P 191, vol. 4, pp. 1238-1260.
7. J. J. Gregory, R. Mata, and N. R. Keltner, Thermal Measurements in a Series of Large Pool Fires, SAND85-0196, Sandia National Laboratories, Albuquerque, New Mexico, 1987.
8. B. F. Blackwell, R. W. Douglas, and H. Wolf, A User's Manual for the Sandia One-Dimensional Direct and Inverse Thermal(SODDIT) Code, SAND85-2478, Sandia National Laboratories, Albuquerque, New Mexico, 1985.
9. P. T. Harsha, W. N. Bragg, and R. B. Edelman, A Mathematical Model of a Large Open Fire, Science Applications Incorporated, NASA Contract Report No. NAS2-10675.
10. R. C. Corlett, Velocity Distributions in Fires, in: Heat Transfer in Fires, John Wiley and Sons, New York, 1974, pp. 239-255.
11. A. M. Birk, and P. H. Oosthuizen, Model for the Prediction of Radiant Heat Transfer to a Horizontal Cylinder Engulfed in Flames, ASME Paper 82-WA/HT-52, 1982.
12. M. E. Schneider, and L. A. Kent, Measurements of Gas Velocities and Temperatures in a Large Open Pool Fire, SAND87-0095C, Sandia National Laboratories, Albuquerque, New Mexico, 1987, (to be presented at the 1987 ASME Heat Transfer Conference, Pittsburgh, PA.)